

Processing and ballistic performance of lightweight armors based on ultra-fine-grain aluminum composites

Timothy (Zhigang) Lin · Quan Yang ·
Chuhu Tan · Bob Liu · Adolphus McDonald

Received: 12 March 2008 / Accepted: 28 August 2008 / Published online: 23 September 2008
© Springer Science+Business Media, LLC 2008

Abstract Over last few decades, Al-based metal matrix composites (MMCs) have become a promising material of choice for lightweight armors in vehicles. Recent development in ultra-fine-grain and nanostructured material technology provides a new opportunity for the substantial strength enhancement of MMCs unattainable with the conventional microstructure of microscale, leading to significant weight reduction in armor packages. In this article, we will present the latest development of a novel class of nanostructured metal matrix composites (NMMCs) based on submicron SiC particulates reinforced nanocrystalline Al alloys. The successful fabrication of large-dimension NMMCs plates with a cost-effective synthesis and consolidation process that can be scaled up for mass production will be demonstrated. The microstructure, processing, mechanical properties, and their correlations of this class of NMMCs will also be reported. The ballistic performance of the NMMCs is investigated through a real test of high-speed machinegun bullets, and a numerical modeling as well.

Introduction

Al-based metal matrix composites (MMCs), particularly ceramic particles reinforced Al alloys, are attractive candidates for lightweight armor materials on account of their

advantages including higher specific strength and stiffness, higher impact/damping properties, and better fatigue resistance as compared with conventional Al alloys [1–3]. Recent development in ultra-fine-grain (UFG) and nanostructured metal matrix composites (UFGMMCs/NMMCs) has exhibited a new type of matrix microstructure with UFG and/or nanometer-size grain for future development of Al-based MMCs, as the greater majority of the composite strength can be contributed by the inherent matrix strength [1–4]. The development of a cost-effective processing method has been one primary focus in the research of UFG/nanostructured materials aimed for commercial applications. Cryomilling, a mechanical attrition of a mixture of ceramics and Al powders within a cryogenic medium (e.g., liquid nitrogen), has been demonstrated as a feasible low-cost method to synthesize UFGMMCs/NMMCs with the ceramic particles uniformly distributed in the nanocrystalline matrix [5]. However, presently most works on cryomilled UFGMMCs/NMMCs have been limited to small-scale fabrications for scientific/academic research, and the consistency/repeatability of the large-scale processing and performance of UFGMMCs/NMMCs has yet to be fully demonstrated.

On the other hand, to enable the potential applications of such Al-based UFGMMCs/NMMCs for lightweight armors, the evaluation of their high-speed impact behaviors and particularly their ballistic performance are necessary. A numerical modeling that can be used to accurately describe or predict these behaviors and performances are desirably needed, in order to save large time and cost consumption generally required in real ballistic tests. At present, although Johnson–Cook’s model [6] has been used extensively in simulating the ballistic behavior of metallic materials, the direct use of this model for the ballistic behavior of MMCs has not yet been successfully proved, on account of the more

T. Lin (✉) · Q. Yang · C. Tan · B. Liu
Aegis Technology Inc., 3300-A Westminster Avenue,
Santa Ana, CA 92703-1442, USA
e-mail: timlin@aegistech.net

A. McDonald
U.S. Army Aviation and Missile Command, Bldg. 5400,
Redstone Arsenal, Huntsville, AL 35898, USA

complicated microstructure generally consisting of metallic matrix and particulate ceramic reinforcement. In this research, a modified Johnson–Cook’s model that takes the effects of ceramic particulate reinforcement into consideration has been established, showing good agreement with the real ballistic test results.

Materials processing and characterization

Processing

A four-step process of cryomilling, degassing, hot isostatic pressing, and secondary processing such as forging (Fig. 1) has been used to produce bulk Al-based NMMC samples. A reliable scalable processing procedure has been established through an extensive study of processing parameters and the associated optimization.

In the development of the NMMCs, one main focus is processing parameters optimization. AA2024Al + 25 wt.% SiC, with SiC particles in the submicron size, has been chosen as the material system for our optimization study. Through extensive experiments, the optimal processing parameters have been identified. Table 1 lists some processing parameters (ranges) related to cryomilling and the subsequent consolidation of cryomilled powders.

Good repeatability/consistency in both microstructure and properties has been achieved using these processing parameters to produce large-dimension ingot samples of 8 in. in diameter.

Characterization

The microstructure evolution during processing has been studied by both SEM and TEM. It is shown from Fig. 2

that cryomilled powders have nano-scale microstructure (20–50 nm) and consolidated bulk composites have nano-scale/UFG microstructure. Although the grain size of consolidated NMMCs (Fig. 2c, d) is larger than that of cryomilled powders (Fig. 2a, b) because of the grain growth during degassing/HIPing, the grain size of consolidated samples are in the ranges of 50–200 nm that goes into the regime of UFG. This observation indicates the good thermal stability of the NMMCs, which has also been reported by other researchers [5, 7].

The formation of nanometer grain size is also confirmed by XRD measurement of the full width at half maximum (FWHM) values for the Al matrix, namely α -Al peaks (Fig. 3). The grain size, more accurately, volume-averaged crystallite size (d) of the cryomilled sample, was determined by analyzing the broadening of XRD peaks and the angular dependence [8]. Specifically, the FWHM values for the α -Al peaks were used for the average grain size calculation. An example is given in Fig. 3a to illustrate the FWHM values for an α -Al peak of the as-received sample (before milling) and the cryomilled sample (after milling), showing that the fcc Al peaks broadened significantly after the milling. The α -Al peaks of the milled mixture are much broader as compared to the sharp and narrow peaks of the starting (as-received) powders, indicating a finer microstructure formed in the sample.

The peak broadening was caused by the small size of the diffracting grains and by the lattice strain (rms strain $\langle e^2 \rangle^{1/2}$). Based on the measurement of FWHM, the average grain size was estimated by using the Scherrer method. Approximating the grain size broadening profiles by a Cauchy function and strain broadening profiles by a Gaussian function, one can find the relationship between d and $\langle e^2 \rangle^{1/2}$ according to the following equation [8]:

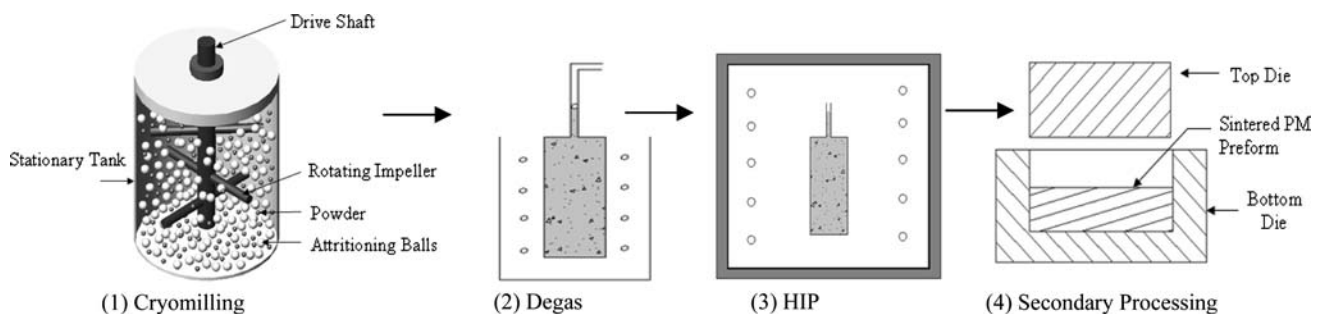


Fig. 1 Schematic of cryomilling and powder consolidation processes

Table 1 Some processing parameters (ranges) related to cryomilling and consolidation

Milling temperature (°C)	Milling speed (rpm)	Milling time (h)	Ball-to-powder ratio	Degassing temperature (°C)	HIPing temperature (°C)	HIPing time (h)
–130 to –160	125–205	5–9	30:1	250–300	390–450	1

Fig. 2 Microstructures in the processing of NMMCs. (a) SEM of cryomilled powder showing ultra-fine particles embedded in large particles; (b) TEM of cryomilled powder showing nanometer-sized grain microstructure; (c) SEM of consolidated bulk composite showing that the matrix has UFG structure; and (d) TEM of consolidated bulk composite showing 100–200 nm grain size

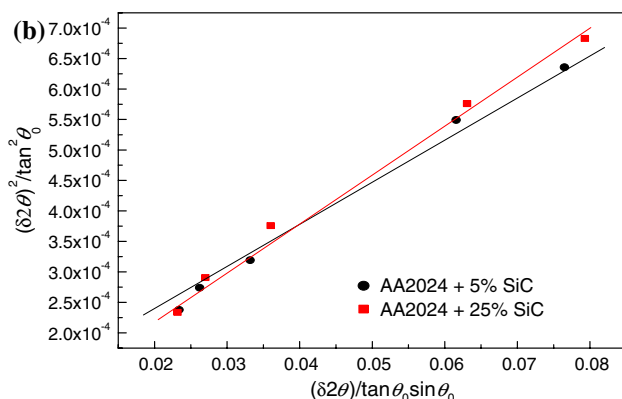
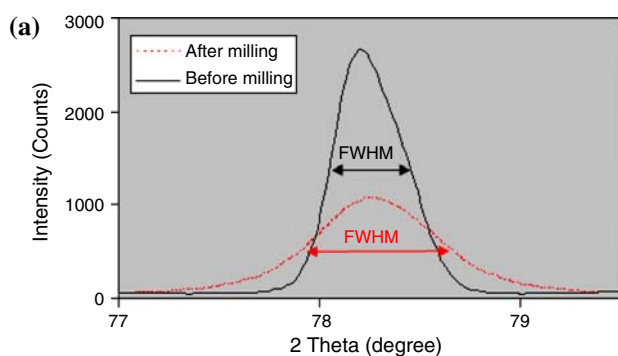
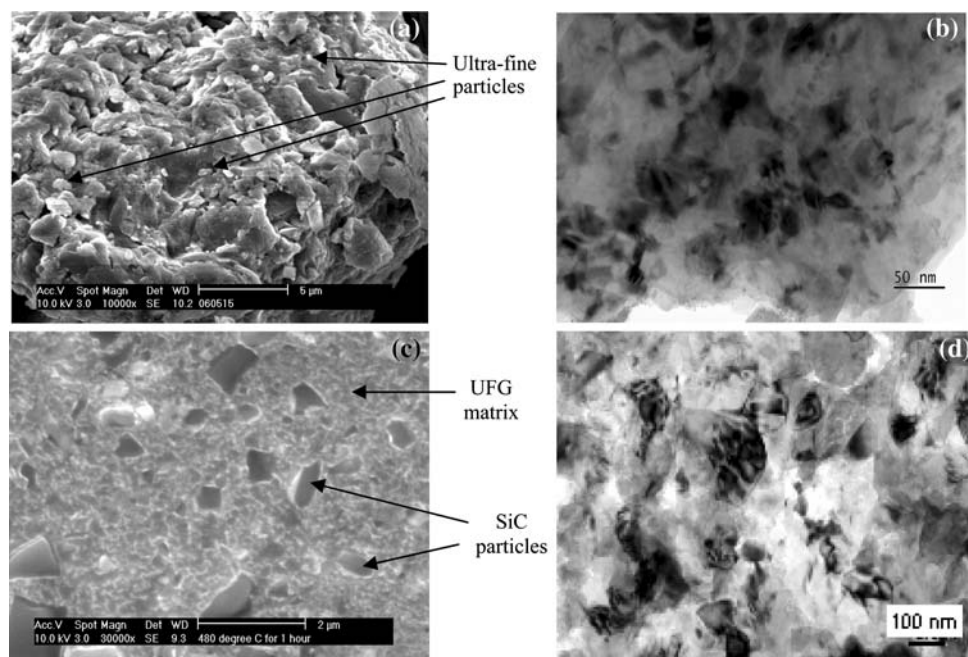


Fig. 3 (a) X-ray diffraction patterns showing the grain size measurement based on the measurement of FWHM of α -Al peaks in the SiC/Al samples and (b) plot used to calculate the grain size

$$\frac{(\delta 2\theta)^2}{\tan^2 \theta_0} = \frac{\lambda}{d} \left(\frac{\delta 2\theta}{\tan \theta_0 \sin \theta_0} \right) + 25 \langle e^2 \rangle \quad (1)$$

where $\delta 2\theta$ is the measured integral breadth, θ_0 is the position of the peak maximum. By performing a least-square-fit to $(\delta 2\theta)^2 / \tan^2 \theta_0$ plotted against $(\delta 2\theta) / \tan \theta_0 \sin \theta_0$ for all of the measured peaks of a sample, d and $\langle e^2 \rangle^{1/2}$ can be determined. Standard linear regression techniques were used to provide an estimate for the uncertainty in the parameters from the error in the fit. The example plots for two as-milled samples are shown in Fig. 3b. Based on the FWHM measurement, the average grain size is estimated in the regime of 20–30 nm for cryomilled powders, and around 100–150 nm for bulk composite samples, which shows good agreement of the observation by TEM measurement.

Compression tests were conducted to obtain the strength, modulus, and elongation of bulk 2024Al-SiC NMMC prototypes, which are also necessary material property inputs in the subsequent analysis of ballistic behaviors. These tests were performed at room temperature in compliance with ASTM standard E9, with specimen dimensions of $4 \times 4 \times 8$ mm. The average ultimate strength is about 660 MPa, modulus is around 110 GPa, and ultimate strain is around 9%.

Ballistic performance results and discussion

The ballistic performance of the Al-based NMMCs fabricated by the processing method introduced in previous section has been evaluated both experimentally and numerically.

Experiments and results

In the experiments, forged NMMC samples are tested against machine gun bullets, which is the kind of bullets that NMMC materials are developed to withstand in the real situation. In general, the ballistic performance of a material is described in terms of the penetration depth by certain penetrators or projectiles to characterize the protection capability of targeted armors. In this article, we emphasize on the protection capacity of armors made by NMMCs. The penetration process typically involves transient impact or rapid plastic deformation under high loading rate conditions and therefore is a complicated process. During penetration, a penetrator defeats armor by tunneling a crater through the target, and the local strain rate can exceed $10^6/s$ with associated strain energies and superimposed stresses that can be significantly greater than the yield strength of the armor material. As a result, the armor material surrounding the crater is pushed aside by the penetrator, while the penetrator itself is forced backwards or back extruded and eroded at the moving boundary between the penetrator and the target. This process continues until the penetrator is either decelerated to a complete stop or completely consumed.

The penetration depths of NMMCs under a high-speed machine gun bullet are investigated. The samples (8 in. in diameter and 2 in. in thickness) were fabricated at large scale using the processing method introduced in last section. The ballistic tests were conducted at Aviation Applied Technology Directorate facility at Ft. Eustis, Virginia, subjected to the penetration of a 50 caliber bullet with the velocity of 450–475 m/s. The resultant penetration depth is 24.3 mm on the average (Fig. 4 shows a typical tested



Fig. 4 A representative picture of a tested specimen

sample), which can be translated into an areal density of 13.4 lbs/ft^2 (areal density is a unit used to compare the ballistic performance of an armor material). The areal density of the NMMCs is around 45% of that of conventional steel armor materials under similar ballistic testing conditions, suggesting this NMMCs armor only needs around 45% of the weight of a steel armor to provide similar ballistic protection.

Analysis and modeling

A modified material strength model is developed to predict and analyze the ballistic performance of this composite, which combines Johnson–Cook's model [6] with the analytic model proposed by Li and Ramesh [9]. The major feature of this model is the incorporation of the reinforcement effects of ceramic particles into the conventional Johnson–Cook's model. In this modified model, the equivalent von Mises stress σ_{eq} is given by

$$\sigma_{eq} = g(f)[A + B\epsilon^n][1 + C \ln \dot{\epsilon}^*][1 - T^{*m}] \quad (2)$$

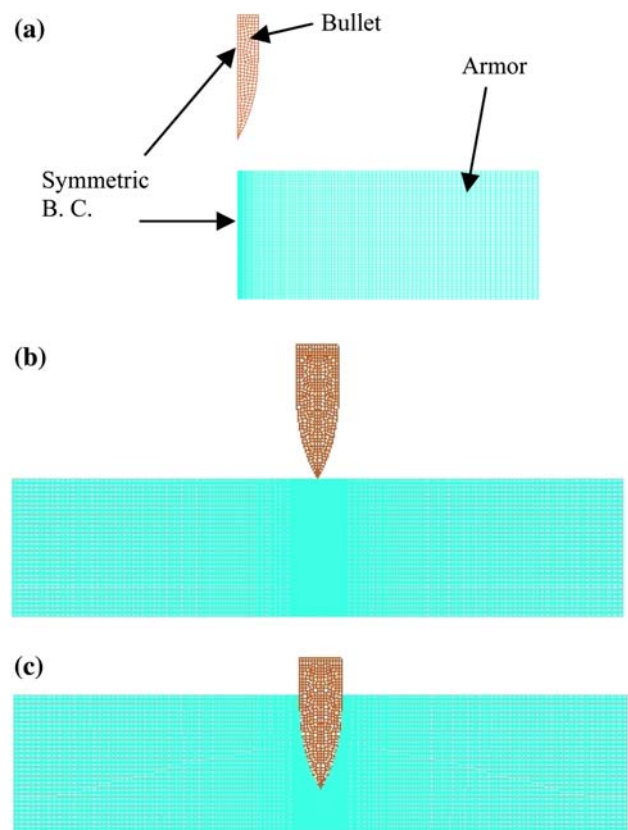


Fig. 5 Ballistic performance modeling using a 50 caliber bullet: (a) illustrations of model geometries; (b) the bullet reaches the armor surface at a speed of 472 m/s; and (c) maximum penetration depth is reached at $t \approx 131 \mu\text{s}$

Table 2 Summary of real test and modeling of NMMCs armor plates penetrated by a machine gun bullet

Specimen no.		E (GPa)	Yield stress (MPa)	Failure stress (MPa)	Armor geometry (mm)	Projectile velocity (m/s)	Penetration depth (mm)	Error (%)
52	Real test	~110	~580	~690	92 R × 41 T	472	~26.8	7.3
	Model	110	580	690			28.7	
53	Real test	~110	~580	~690	95 R × 43 T	452	~24.0	8.6
	Model	110	580	690			26.0	
54	Real test	~110	~580	~690	98 R × 52 T	456	~22.8	2.4
	Model	110	580	690			22.3	

where $g(f)$ is a factor that reflect the ceramic particle influence on the strength of ceramic particle reinforced UFGMMCs/NMMCs via volume fraction f , particle shape, etc. A represents yield stress, B and n are strain hardening parameters, C represents viscous effect, ε is the equivalent plastic strain, $\dot{\varepsilon}^* = \dot{\varepsilon}/\dot{\varepsilon}_0$ is a dimensionless strain rate, and $\dot{\varepsilon}_0$ is a reference strain rate, $T^* = (T - T_0)/(T_m - T_0)$ is the homologous temperature, where T is the absolute temperature, T_0 is the room temperature, and T_m is the melting temperature of the target material, respectively. The corresponding damage model is adopted from that of Johnson–Cook [6].

The modified model described by Eq. 1 has been successfully implemented in LS-DYNA, a non-linear finite element code for analysis of large deformation dynamic response of structures based on explicit time integration. The density of the NMMCs is estimated to be around 2800 kg/m³ based on the weight percentage of SiC particles. A yield stress of 580 MPa and failure stress around 690 MPa are used according to mechanical test results of the NMMCs, and cylindrical particle shape is assumed for SiC reinforcement.

The modeling of ballistic performance penetrated by a 50 caliber bullet is illustrated in Fig. 5. A representative geometry of a machine gun bullet (half section) and an armor plate (half section) in the simulation is shown in Fig. 5a, where the armor plate has a dimension of 184 mm in diameter and 41 mm in thickness from a real test sample. Considering the symmetric boundary conditions (B. C.) of both the bullet and the armor along the centerline, only an half section of the bullet and the armor plate are shown. Figure 5b shows the machine gun bullet reaches the armor surface at a speed of 472 m/s in the simulation, and the maximum penetration depth of 28.7 mm is reached at $t \approx 131 \mu\text{s}$ (Fig. 5c). In the real ballistic test, the penetration depth is about 26.8 mm.

Comparisons between the real tests and the simulation results are summarized in Table 2. As can be seen, the penetration depth of simulation obtained from the modified ballistic model agrees very well with those from real tests, with a deviation less than 10%.

Conclusion

A novel class of MMCs based on submicron SiC particulates reinforced UFG and nanostructured material Al alloys, which is referred to as NMMCs, has been investigated with focus on the establishment of large-quantity processing and evaluation of ballistic performances of this class of material. The fabrication of large-dimension NMMC plates by using a cost-effective synthesis and consolidation process that can be scaled up for mass production is demonstrated. Good repeatability/consistency in both microstructure and properties has been achieved. A modified Johnson–Cook's model has been established and successfully used to evaluate the ballistic behaviors of the NMMCs under high-speed bullets, which shows a considerably good agreement between modeling and real test results.

Acknowledgement This work was funded by the U.S. Army Small Business Innovation Research (SBIR) project (contract no.: W911W6-06-C-0032).

References

- Chawla KK (1993) In: Chou TW (ed) Materials science and technology, vol 13: structure and properties of composites. VCH, Weinheim, p 121
- Park KT, Lavernia EJ, Mohamed FA (1994) Acta Metall Mater 42:667. doi:10.1016/0956-7151(94)90264-X
- Park KT, Mohamed FA (1995) Metall Mater Trans A 26A:3119. doi:10.1007/BF02669441
- Fecht HJ, Ivanisenko Y (2007) In: Koch CC (ed) Nanostructured materials: processing, properties, and applications, chapter 4: nanostructured materials and composites prepared by solid state processing, 2nd edn. William Andrew Pub, Norwich, NY, p 119
- Witkin DB, Lavernia EJ (2006) Prog Mater Sci 51:1. doi:10.1016/j.pmatsci.2005.04.004
- Johnson GR, Cook WH (1985) Eng Fract Mech 21(1):31. doi:10.1016/0013-7944(85)90052-9
- Malow TR, Koch CC (1997) Acta Mater 45(5):2177. doi:10.1016/S1359-6454(96)00300-X
- Klug HP, Alexander L (1974) X-ray diffraction procedures for polycrystalline and amorphous materials, 2nd edn. Wiley, New York, p 661
- Li Y, Ramesh KT (1998) Acta Mater 46(16):5633. doi:10.1016/S1359-6454(98)00250-X